ELSEVIER

Coordination Chemistry Reviews
197 (2000) 231–247

COORDINATION CHEMISTRY REVIEWS

www.elsevier.com/locate/ccr

Geometry and binding strength of a π-type hydrogen-bonded complex of ethene and hydrogen bromide determined by rotational spectroscopy

P.W. Fowler, A.C. Legon *, J.M.A. Thumwood, E.R. Waclawik

School of Chemistry, University of Exeter, Stocker Road, Exeter EX4 4QD, UK

Received 24 February 1999; accepted 25 May 1999

Contents

Abstract

The ground-state rotational spectra of the four isotopomers $C_2H_4\cdots H^{79}Br$, $C_2H_4\cdots H^{81}Br$, $C_2H_4\cdots D^{79}Br$ and $C_2H_4\cdots D^{81}Br$ of an asymmetric-top complex formed by ethene with hydrogen bromide were observed by pulsed-nozzle, Fourier-transform, microwave spectroscopy. A fast-mixing nozzle was used to preclude any reaction induced by formation of Br atoms on vessel walls. Large Br nuclear quadrupole hyperfine splittings combined with HBr subunit angular oscillations of wide amplitude allowed the detection of centrifugal distortion effects on the hyperfine patterns. These effects were manifest in a dependence of χ_{aa} on K_{-1} through a term $\chi_K K^2_{-1}$ and in an additional term $\chi_d\ K^2_{-1}\ (4\ K^2_{-1}-1)/\{J(J+1)\}$ in the

* Corresponding author. Tel.: +44-1392-263488; fax: +44-1392-263434.
E-mail address: a.c.legon@exeter.ac.uk (A.C. Legon)

PII: S0010-8545(99)00197-6

quadrupole energy expression. The set of spectroscopic constants A_0, B_0, C_0, Δ_J, Δ_{JK}, δ_J, χ_{aa}, $\chi_{bb}-\chi_{cc}$, χ_K, χ_d, M_{aa} and $M_{bb}=M_{cc}$ was determined for each isotopomer investigated. Detailed analyses of various spectroscopic constants showed that, in the $C_2H_4\cdots HBr$ complex, the HBr subunit forms a weak hydrogen bond to the centre of the π-bond of ethene, as characterised by an intermolecular stretching force constant $k_\sigma = 5.2$ Nm^{-1}. In the equilibrium form of the complex, the HBr subunit therefore lies along the C_2 axis of ethene that is perpendicular to the nuclear plane. In the zero-point state, the distance from the centre (*) of the π bond to Br is $r(*\cdots Br) = 3.916$ (4) Å. Systematic behaviour of distances $r(Z\cdots X)$, where Z is the electron donor atom or centre of B, and of k_σ values in the series $B\cdots HX/B\cdots XY$, where X = Br or Cl and Y = Cl, is discussed.

Keywords: Rotational spectroscopy; Radial and angular geometry; Type and strength of interaction

1. Introduction

We report the detection and characterisation of a complex formed between ethene and hydrogen bromide in the gas phase. This was achieved through analysis of the ground-state rotational spectra of the four isotopomers $C_2H_4\cdots H^{79}Br$, $C_2H_4\cdots H^{81}Br$, $C_2H_4\cdots D^{79}Br$, and $C_2H_4\cdots D^{81}Br$, as observed with a pulsed-nozzle, Fourier-transform instrument that incorporated a fast-mixing nozzle [1] to preclude chemical reaction between the components. The investigation has several aims. The first is to identify the type of interaction in the lowest energy form of the complex, i.e. whether HBr forms a hydrogen bond to the π-electrons of ethene or whether the dispersion interaction of Br and ethene is predominant. The second aim is to determine the precise radial and angular geometry of the complex, while the third is to obtain a measure of the strength of the interaction.

There are two particular reasons for interest in $C_2H_4\cdots HBr$. First, there is the challenge of observing the lowest energy species formed from the interaction of the components in a system that features prominently in the discussion of the addition of hydrogen halides to alkenes. Mixing of HBr and ethene under conditions likely to lead to formation of Br atoms on surfaces (such as in the stainless steel tanks used to pre-mix component gases in the type of spectroscopy described here) encourages free-radical (anti-Markownikov) addition. The fast-mixing nozzle allows complexes to be formed in the absence of surfaces, avoids Br atom production and therefore suppresses the free radical mechanism.

The second reason for special interest in $C_2H_4\cdots HBr$ lies in the distance $r(*\cdots Br)$ between the centre of the C=C bond and the Br atom and its relationship to the corresponding distance in the complex $C_2H_4\cdots BrCl$. The pair $C_2H_4\cdots HBr/C_2H_4\cdots BrCl$ is a member of the series $B\cdots HBr/B\cdots BrCl$ that is being investigated systematically to find whether the contraction Δr in the distance $r(Z\cdots Br)$ between $B\cdots HBr$ and $B\cdots BrCl$ is independent of B, where Z is the acceptor atom or centre in B. The experimental findings [2], that $\Delta r = 0.53(7)$Å in several members of the series $B\cdots HCl/B\cdots Cl_2$ led to the suggestion that the contraction reflects the 'snub-nosed' nature of the Cl atom in Cl_2 [3], i.e. the Van der Waals radius of Cl is

smaller along the internuclear axis than perpendicular to it. A similar contraction of $\Delta r = 0.88$ (11) Å has been observed for the corresponding series B···HCl/B···ClF [4]. Model calculations, in which the helium atom was used to probe the repulsive potential of Cl_2 and ClF, reveal that such an anisotropy indeed exists in these dihalogens and gives Δr for B···HCl/B···Cl_2 and B···HCl/B···ClF in good agreement with experiment [5]. Δr has been measured for only a few members of the B···HBr/B···BrCl series. The present work on C_2H_4···HBr, in combination with existing results for C_2H_4···BrCl, leads to Δr for B = C_2H_4.

2. Experimental

Ground-state rotational spectra of the four isotopomers C_2H_4···$H^{79}Br$, C_2H_4···$H^{81}Br$, C_2H_4···$D^{79}Br$ and C_2H_4···$D^{81}Br$ were observed by means of a pulsed-nozzle, Fourier-transform, microwave spectrometer [6,7]. Instead of pre-mixing ethene and hydrogen bromide in the conventional stagnation tank and risking reaction through the production of Br atoms, a fast-mixing nozzle was employed. The construction of the nozzle has been described elsewhere [1]. Ethene (Aldrich) was flowed continuously through the inner of the two concentric, co-terminal tubes to give a nominal pressure of 1×10^{-4} mbar in the evacuated Fabry-Pérot cavity, while a 1:100 mixture of HBr in argon was pulsed down the outer tube at a rate of 2 Hz. The stagnation pressure of the room temperature HBr/Ar mixture was 3 bar. Rotational transitions were detected and measured in the conventional way. Individual Br nuclear quadrupole hyperfine components in C_2H_4···HBr had a full-width at half height of ca. 20 kHz and were measured with an estimated accuracy of 2 kHz. Hyperfine components in the C_2H_4···DBr isotopomers were broadened and, occasionally, partially resolved as a result of the additional D nuclear quadrupole interaction. The centre of gravity of partially resolved structure was then taken. Consequently, the estimated accuracy for C_2H_4···DBr species is somewhat larger.

DBr gas was prepared by dehydration of a solution of DBr in D_2O (Aldrich, 99.5 atom% D) with phosphorus pentoxide.

3. Determination of spectroscopic constants

The observed ground-state rotational spectra of C_2H_4···$H^{79}Br$ and C_2H_4···$H^{81}Br$ were typical of a nearly prolate, asymmetric rotor carrying a single Br nucleus on the *a* axis. Thus, each $J'_{K_{-1}K_1} \leftarrow J''_{K_{-1}K_1}$ transition exhibited a Br nuclear quadrupole hyperfine structure similar to that expected of the limiting symmetric rotor. Observed frequencies of hyperfine components in several rotational transitions are recorded in Table 1 for these two isotopomers.

In an initial least-squares fit of the hyperfine frequencies to give spectroscopic constants using the program written by Pickett [8], we employed a standard Hamiltonian *H* of the form:

$$H = H_R + H_Q + H_{SR} \quad (1)$$

which was constructed in the coupled basis $\boldsymbol{I} + \boldsymbol{J} = \boldsymbol{F}$. In Eq. (1), H_R is appropriate to a semi-rigid asymmetric rotor, H_Q describes the Br nuclear quadrupole interaction through the operator $-1/6$ **Q**: ∇**E** in terms of the Br nuclear electric quadrupole tensor **Q** and the electric field gradient tensor ∇**E**, and $H_{SR} = \boldsymbol{I}\cdot\mathbf{M}\cdot\boldsymbol{J}$, where **M** is the spin-rotation coupling tensor. For H_R, the Watson A reduction in the I^r representation was employed, but only quartic centrifugal distortion constants were necessary and, of those, only Δ_J, Δ_{JK} and δ_J were determinable from the available transitions. Of the components of the Br nuclear quadrupole coupling tensor $\chi_{\alpha\beta} = -(eQ/h)\partial^2 V/\partial\alpha\partial\beta$ ($\alpha,\beta = a,b,c$) only χ_{aa} and $\chi_{bb} - \chi_{cc}$ were nonzero.

The set of spectroscopic constants determined in the initial analyses are given in columns A of Table 2 while the residuals from the final cycle of the least-squares fits are correspondingly in columns A of Table 1. We note that $\chi_{bb} - \chi_{cc} \approx 0$, a result that suggested setting $M_{bb} = M_{cc}$, since the spin-rotation coupling tensor contributes very little to the observed frequencies and these components were not separately well determined. It is clear from the residuals in Table 1 and from the standard deviations σ (Table 2) of the initial fits of both $C_2H_4\cdots H^{79}Br$ and $C_2H_4\cdots H^{81}Br$, which significantly exceed the estimated error (2 kHz) of frequency measurement, that the Hamiltonian of Eq. (1) is inadequate for this complex.

The effects of centrifugal distortion on nuclear quadrupole hyperfine structure in weakly bound complexes can be significant when the complex contains a nucleus associated with a large nuclear quadrupole coupling constant. Such effects have been observed in Ar···HBr [9] and $H_3P\cdots$HBr [10], for example. Hougen [11] has shown that, in the case of a symmetric-top molecule carrying a quadrupolar nucleus on the symmetry axis, centrifugal distortion modifies the hyperfine structure in two ways. First, the coupling constant is no longer independent of rotational state but varies with the quantum numbers J and K according to

$$\chi_{aa} = \chi_R + \chi_J J(J+1) + \chi_K K^2 \quad (2)$$

where χ_R refers to the rotationless state. Secondly, an additional term should be included in the energy expression describing the nuclear quadrupole interaction and this has the form

$$\chi_d[K^2(4K^2-1)/\{J(J+1)\}]\,Y(I,J,F) \quad (3)$$

where $Y(I,J,F)$ is Casimir's function. In view of the close approximation of $C_2H_4\cdots$HBr to the prolate symmetric rotor limit (Ray's $\kappa = -0.994$) and the fact that $\chi_{bb} - \chi_{cc}$ is very close to zero (see Table 2), it is appropriate to allow for the effect of centrifugal distortion on the Br nuclear quadrupole coupling by assuming that χ_{aa} depends on J and K according to Eq. (2) and that any residual contribution can be described by the simple term in Eq. (3), with K replaced by K_{-1}. Hence, in a second analysis, the following procedure was used.

An initial guess at the value of χ_d was made and each frequency was corrected for the contribution calculated from Eq. (3). The corrected frequencies were then fitted using Pickett's program [8] to give A_0, B_0, C_0, Δ_J, Δ_{JK}, δ_J, χ_{aa}, $\chi_{bb} - \chi_{cc}$, χ_K, M_{aa}

Table 1
Observed and calculated frequencies of $C_2H_4\cdots H^{79}Br$ and $C_2H_4\cdots H^{81}Br$

Transition		$C_2H_4\cdots H^{79}Br$			$C_2H_4\cdots H^{81}Br$		
$J'_{K_{-1}K_1} \leftarrow J''_{K_{-1}K_1}$	$2F' \leftarrow 2F''$	ν_{obs} (MHz)	A [a]	B [b]	ν_{obs} (MHz)	A [a]	B [b]
$3_{03} \leftarrow 2_{02}$	3 ← 1	9279.5192	−8.1	−2.9	9217.6992	−7.0	−3.6
	5 ← 3	9278.7212	−4.7	0.2	9217.1419	−1.1	1.4
	7 ← 5	9252.6898	1.4	0.8	9195.3162	1.5	−0.3
	9 ← 7	9252.7813	−0.1	−0.6	9195.3851	5.6	3.1
	3 ← 3	9170.8702	20.2	2.1	9127.0974	15.5	4.5
	5 ← 5	9203.5073	11.3	0.6	9154.1043	8.7	2.5
	7 ← 7	9360.3111	−22.0	0.2	9285.2131	−4.4	11.3
$3_{12} \leftarrow 2_{11}$	3 ← 1	9346.5591	2.3	0.2	–	–	–
	5 ← 3	9373.9752	3.8	3.1	9311.9057	3.0	4.4
	7 ← 5	9373.0719	−0.1	2.2	9311.1637	−0.3	1.5
	9 ← 7	9346.6982	0.2	−0.2	9289.0648	1.1	−0.6
	3 ← 3	9293.4907	−12.3	−3.6	9244.6271	−13.0	−2.4
	5 ← 5	9335.7463	−5.7	−0.2	9279.9299	−9.5	−4.1
	7 ← 7	9427.9209	10.5	−2.8	9356.8578	10.2	−3.5
$3_{13} \leftarrow 2_{12}$	3 ← 1	9144.8658	1.0	−1.1	9089.9181	−10.3	−7.6
	5 ← 3	9172.2630	3.1	2.4	9112.7380	−0.6	1.1
	7 ← 5	9171.4735	−1.6	0.7	9112.0917	0.6	1.9
	9 ← 7	9145.1141	−0.9	−1.3	9090.0032	2.7	0.6
	3 ← 3	9092.1257	−10.9	−2.1	9045.7535	−8.9	−0.7
	5 ← 5	9134.3355	−5.8	−0.3	9081.0147	−2.8	0.7
	7 ← 7	9226.0081	13.8	0.5	9157.5169	10.1	−0.8
$3_{21} \leftarrow 2_{20}$	3 ← 1	9148.5006	−15.6	−0.4	–	–	–
	5 ← 3	9255.6351	7.7	−4.6	–	–	–
	7 ← 5	9332.3355	14.7	−0.3	9261.2615	5.1	−7.7
	9 ← 7	9224.2397	−6.2	2.4	9171.0402	−6.3	0.8
$3_{22} \leftarrow 2_{21}$	3 ← 1	9147.9398	−14.7	1.6	–	–	–
	5 ← 3	9255.0765	12.0	0.8	9196.6295	−3.4	−0.6
	7 ← 5	9331.7730	15.5	1.6	9260.7221	17.9	5.1
	9 ← 7	9223.6751	−8.7	1.1	9170.4812	−14.0	−6.9
$4_{04} \leftarrow 3_{03}$	5 ← 3	12351.8268	−5.2	−2.5	12272.7319	−3.1	−1.9
	7 ← 5	12351.6108	−4.0	−1.4	12272.5784	−3.0	−2.5
	9 ← 7	12339.4083	−0.6	−0.5	12262.3537	4.3	2.4
	11 ← 9	12339.4550	−3.0	−2.9	12262.3812	−2.2	−4.8
	5 ← 5	12243.9773	21.2	1.0	12182.6885	14.5	2.2
	7 ← 7	12302.4285	6.2	−1.4	12231.3670	4.7	0.8
	9 ← 9	12446.9389	−21.9	1.0	12352.1641	−23.3	−6.9
$4_{13} \leftarrow 3_{12}$	5 ← 3	12475.7383	1.4	0.4	12396.6637	−1.7	−0.6
	7 ← 5	12486.6700	3.1	2.5	12405.7714	1.6	1.7
	9 ← 7	12481.0406	1.8	2.3	12401.0712	0.3	0.1
	11 ← 9	12470.5083	0.7	0.0	12392.2458	2.4	0.1
$4_{14} \leftarrow 3_{13}$	5 ← 3	12206.9350	1.3	−0.1	12131.2302	−5.9	−2.7
	7 ← 5	12217.8638	1.0	−0.1	12140.3381	−1.7	0.5
	9 ← 7	12212.2848	2.0	1.9	12135.6784	−1.3	0.1
	11 ← 9	12201.7581	0.7	−0.5	12126.8564	0.1	−0.5
	7 ← 7	12180.7310	2.0	4.1	–	–	–
	9 ← 9	–	–	–	12203.1975	11.5	4.1
$4_{22} \leftarrow 3_{21}$	11 ← 9	12324.2939	−6.6	−3.8	–	–	–
$4_{23} \leftarrow 3_{32}$	11 ← 9	–	–	–	12247.8702	2.5	8.0

[a] Residuals $\Delta\nu = \nu_{obs} - \nu_{calc}$ for the final cycle of the fit to the standard Hamiltonian described by Eq. (1). [b] Residuals $\Delta\nu = \nu_{obs} - \nu_{calc}$ for the final cycle of the fit to the Hamiltonian which includes the χ_κ term described by Eq. (2) and the χ_d term described by Eq. (3).

Table 2
Determined spectroscopic constants of $C_2H_4\cdots HBr$ and $C_2H_4\cdots DBr$

Spectroscopic constant	$C_2H_4\cdots H^{79}Br$		$C_2H_4\cdots H^{81}Br$		$C_2H_4\cdots D^{79}Br$		$C_2H_4\cdots D^{81}Br$	
	A	B	A	B	A	B	A	B
A_0 (MHz)	25625(24)	25580(24)	25484(26)	25485(26)	25531(26)	25576(27)	25673(27)	25695(28)
B_0 (MHz)	1576.72538(53)	1576.72536(53)	1566.60147(55)	1566.60117(55)	1579.86386(51)	1579.86461(52)	1569.64995(56)	1569.65030(56)
C_0 (MHz)	1509.51634(50)	1509.51616(50)	1500.23196(51)	1500.23247(51)	1512.52381(49)	1512.52393(49)	1503.15964(53)	1503.15987(53)
Δ_J (kHz)	3.6144(71)	3.6040(71)	3.5382(77)	3.5371(78)	3.4483(74)	3.4710(75)	3.4129(77)	3.4291(78)
Δ_{JK} (kHz)	174.762(63)	174.848(63)	172.575(58)	172.754(59)	167.052(76)	167.018(89)	164.454(85)	164.324(94)
δ_J (kHz)	0.1500(89)	0.1522(89)	0.1618(91)	0.1520(91)	0.1563(85)	0.1650(85)	0.1421(92)	0.1429(92)
χ_{aa} (MHz)	429.7127(28)	429.6219(37)	358.9922(30)	358.9317(37)	447.4627(31)	447.3986(35)	373.8080(31)	373.7662(38)
$\chi_{bb}-\chi_{cc}$ (MHz)	−1.3835(81)	−1.3837(81)	−1.1462(77)	−1.1596(77)	−0.9665(69)	−0.9731(69)	−0.7900(75)	−0.8086(75)
χ_K (MHz)	–	0.1274(15)	–	0.095(24)	–	0.1167(30)	–	0.0883(33)
χ_d (MHz)	–	−0.062	–	−0.040	–	−0.060	–	−0.060
M_{aa} (kHz)	1.1(11)	−4.5(11)	7.7(13)	−4.0(14)	−4.7(13)	−4.3(14)	−13.9(19)	−6.9(21)
M_{bb} [a] (kHz)	2.38(18)	2.38(33)	0.98(18)	1.67(35)	1.21(17)	1.80(17)	1.87(18)	1.85(19)
N [b]	46	46	42	42	42	42	38	38
σ (kHz) [c]	9.4	1.9	8.0	3.9	8.1	2.9	6.2	3.1

[a] It is assumed that $M_{bb} = M_{cc}$ in the fit.
[b] Number of hyperfine components in fit.
[c] Standard deviation of fit.

and $M_{bb} = M_{cc}$. It was found that the term χ_J in Eq. (2) contributed negligibly and it was set to zero. This procedure was repeated until the value of χ_d was found that minimised the standard deviation of the fit. The resulting sets of spectroscopic constants for $C_2H_4\cdots H^{79}Br$ and $C_2H_4\cdots H^{81}Br$ are given in columns B in Table 2. The residuals appropriate to these spectroscopic constants are given in columns B of Table 1. It should be noted that the fit is now satisfactory and that the coefficients χ_K and χ_d are small, well determined and, within experimental error, scale according to the ratio, $^{79}Q/^{81}Q = 1.197048(3)$, of the Br nuclear electric quadrupole moments [12].

The set of spectroscopic constants obtained by applying an identical procedure to the frequencies of the isotopomers $C_2H_4\cdots D^{79}Br$ and $C_2H_4\cdots D^{81}Br$ (see Table 3) is included in Table 2. The values of χ_K and χ_d are similar to those of the HBr isotopomers.

4. Symmetry and geometry of the complex

The determined rotational constants of the four observed isotopomers of $C_2H_4\cdots HBr$ allow some firm conclusions about the symmetry and geometry of the complex.

First, we note that the rotational constant A_0 has a similar magnitude for each of the isotopomers and that this value is a few per cent larger than C_0 of the free ethene molecule, the ground-state rotational constants [13] of which are collected in Table 4, for convenience. These observations are consistent with an equilibrium geometry of $C_2H_4\cdots HBr$ of the type shown in Fig. 1, i.e. one with C_{2v} symmetry and in which the HBr internuclear axis coincides with the C_2 axis of free ethene that is perpendicular to its nuclear plane.

The reason that A_0 of the complex is greater in magnitude than C_0 of ethene is readily understood. In the zero-point state of the complex the two subunits C_2H_4 and HBr undergo angular oscillations pivoted at their respective mass centres. The motion of the HBr subunit involves mainly the H atom because the HBr centre of mass is very close to Br. The motion of the C_2H_4 subunit that can affect A_0 is an oscillation about its C_2 axis that lies parallel to the c axis of the complex (Fig. 1). This motion can only cause A_0 to be larger than the equilibrium value and, hence, than C_0 of free ethene.

The planar moments P_α of the four isotopomers investigated are given in Table 5 and are defined by

$$P_\alpha = (1/2)(I_\beta + I_\gamma - I_\alpha) = \sum_i m_i \alpha_i^2 \tag{4}$$

where α, β and γ are to be permuted over, a, b and c. If the equilibrium geometry of the complex were as shown in Fig. 1, then the equilibrium values of P_b and P_c would be identical to the corresponding quantities P_a^E and P_b^E of free ethene (E), respectively. Table 5 includes the zero-point values of the P_α^E [13] and it may be seen that P_a^E is nearly equal to P_b of the complex. The small difference $P_b^E - P_c$ can

Table 3
Observed and calculated frequencies of $C_2H_4\cdots D^{79}Br$ and $C_2H_4\cdots D^{81}Br$

Transition		$C_2H_4\cdots D^{79}Br$			$C_2H_4\cdots D^{81}Br$		
$J'_{K_{-1}\,K_1} \leftarrow J''_{K_{-1}\,K_1}$	$2F' \leftarrow 2F''$	ν_{obs} (MHz)	A [a]	B [b]	ν_{obs} (MHz)	A [a]	B [b]
$3_{03} \leftarrow 2_{02}$	3 ← 1	9298.8960	5.7	8.7	9236.4128	7.2	8.9
	5 ← 3	9298.0196	−2.1	0.0	9235.7956	−1.4	0.1
	7 ← 5	9270.9274	−3.2	−5.5	9213.0811	−3.9	−4.8
	9 ← 7	9271.0339	4.5	1.6	9213.1608	5.2	4.2
	3 ← 3	9185.6902	15.5	2.9	9142.0187	14.7	5.6
	5 ← 5	9219.7549	5.8	−1.6	9170.1973	8.5	2.8
	7 ← 7	9383.0192	−16.0	−0.4	9306.6943	−7.4	2.0
$3_{12} \leftarrow 2_{11}$	3 ← 1	9364.7410	1.5	−1.3	–	–	–
	5 ← 3	9393.3156	6.5	3.4	9330.6103	2.0	−3.4
	7 ← 5	9392.3841	1.6	1.9	9329.8500	−3.1	−3.1
	9 ← 7	9364.9385	−0.2	−1.2	9306.8554	−4.5	−4.2
	3 ← 3	9309.5825	−9.8	2.9	9260.6242	−7.5	3.2
	5 ← 5	9353.5541	−15.0	−6.7	9297.3648	−13.0	−4.4
	7 ← 7	9449.4840	10.5	−2.4	9377.4222	13.2	1.1
$3_{13} \leftarrow 2_{12}$	3 ← 1	9162.6858	10.6	8.1	–	–	–
	5 ← 3	9191.2226	−1.9	−4.6	9131.0940	0.3	−4.0
	7 ← 5	9190.3821	−6.0	−5.8	9130.4058	−2.8	−2.8
	9 ← 7	9162.9599	1.1	0.1	9107.4225	−3.1	−2.8
	3 ← 3	9107.7372	−11.0	0.2	9061.3096	−4.4	2.9
	5 ← 5	9151.7055	−8.6	−0.5	9098.0333	−10.0	−3.9
	7 ← 7	9247.2758	10.3	−0.9	9177.7939	7.3	−0.2
$3_{22} \leftarrow 2_{21}$	2 ← 1	9162.2479	−9.5	−1.3	–	–	–
	5 ← 3	9273.7945	16.7	–0.7	–	–	–
	7 ← 5	–	–	–	9281.5364	6.1	1.1
	9 ← 7	9241.0710	−5.6	2.9	9187.5972	−2.6	1.8
$4_{04} \leftarrow 3_{03}$	5 ← 3	12376.8240	−4.3	−2.4	12296.9911	−1.7	−0.3
	7 ← 5	12376.5920	−0.4	0.9	12296.8257	−2.0	−0.6
	9 ← 7	12363.8952	3.6	2.5	12286.1813	−0.4	−0.1
	11 ← 9	12363.9430	0.1	−1.6	12286.2209	1.9	2.2
	5 ← 5	12264.4926	11.2	−1.5	12203.2025	2.8	−6.4
	7 ← 7	12325.4144	3.5	−0.3	12253.9351	3.6	0.2
	9 ← 9	12475.8800	−17.0	0.0	12379.7143	−13.0	−2.8
$4_{13} \leftarrow 3_{12}$	5 ← 3	12500.6240	−3.2	−1.1	12420.8677	1.9	0.0
	7 ← 5	12512.0141	−1.4	0.2	12430.3559	2.9	1.5
	9 ← 7	12506.1570	−2.6	0.2	12425.4681	0.3	1.4
	11 ← 9	12495.1994	−1.7	0.2	12416.2844	−0.5	0.8
	9 ← 9	12590.7053	10.8	1.7	–	–	–
$4_{14} \leftarrow 3_{13}$	5 ← 3	12231.3100	−1.3	−1.0	12154.9518	1.6	0.2
	7 ← 5	12242.6986	−0.1	−0.3	12164.4390	2.2	1.4
	9 ← 7	12236.8790	−0.3	0.5	12159.5813	1.0	2.0
	11 ← 9	12225.9273	0.5	0.4	12150.4009	−0.8	0.5
	7 ← 7	12204.0174	−7.3	0.5	12132.0649	−7.1	−1.2
	9 ← 9	12321.1966	10.6	1.1	12229.9492	7.9	1.0

[a] Residuals $\Delta\nu = \nu_{obs} - \nu_{calc}$ for the final cycle of the fit to the standard Hamiltonian described by Eq. (1). [b] Residuals $\Delta\nu = \nu_{obs} - \nu_{calc}$ for the final cycle of the fit to the Hamiltonian which includes the χ_K term described by Eq. (2) and the χ_d term described by Eq. (3).

Table 4
Spectroscopic constants of ethene and hydrogen bromide

Spectroscopic constant	C_2H_4 [a]	$H^{79}Br$	$H^{81}Br$	$D^{79}Br$	$D^{81}Br$
A_0(MHz)	145837.75(14)	–	–	–	–
B_0(MHz)	30010.79 (5)	250358.510 [b]	250280.582 [b]	127357.639 [b]	127279.757 [b]
C_0(MHz)	24824.17(5)	250358.510	250280.582	127357.639	127279.757
r_0(Å) [c]	–	1.42426	1.42426	1.42144	1.42144
χ_0(Br)	–	532.3059 [d]	444.6807 [d]	530.6315 [e]	443.2799 [e]

[a] Ref. [13].
[b] Ref. [17].
[c] r_0 values for HBr/DBr were calculated from the B_0 values by using the operational definition $r_0 = \{h/(8\pi^2\mu B_0)\}^{1/2}$.
[d] Ref. [15].
[e] Ref. [16].

be interpreted to give a value of the pseudo-inertia defect for the complex as follows.

We assume that only the intermolecular modes of the complex contribute significantly to the difference $P_b^E - P_c$ and that the ground-state moments of inertia of free ethene can be taken as equilibrium values for present purposes. In that case, P_b^E can be written as

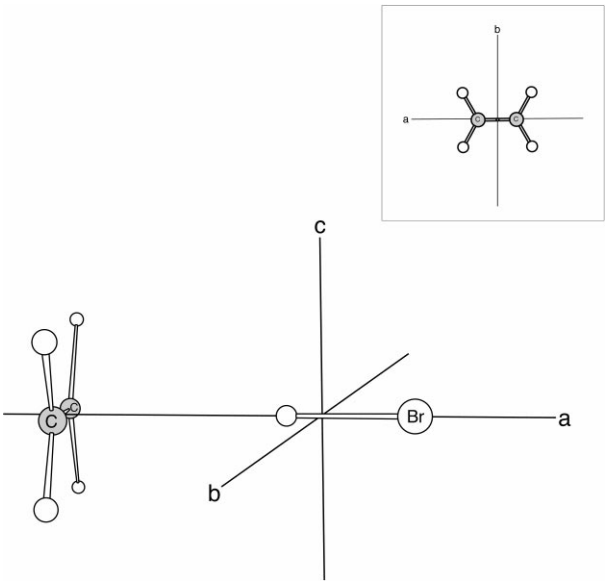

Fig. 1. The equilibrium angular geometry of the complex $C_2H_4\cdots HBr$. The diagram is drawn to scale and the positions of the principal inertia axes *a*, *b* and *c* are indicated. The insert shows the directions of the principal inertial axes *a* and *b* in the free ethene molecule.

Table 5
Planar moments of $C_2H_4\cdots H^{79}Br$, $C_2H_4\cdots H^{81}Br$, $C_2H_4\cdots D^{79}Br$, $C_2H_4\cdots D^{81}Br$ and C_2H_4

Planar moment [a]	$C_2H_4\cdots H^{79}Br$	$C_2H_4\cdots H^{81}Br$	$C_2H_4\cdots D^{79}Br$	$C_2H_4\cdots D^{81}Br$	C_2H_4
P_α (u Å^2)	317.781(9)	319.816(10)	317.128(11)	319.256(11)	0.0531(2)
P_β (u Å^2)	17.014(9)	17.051(10)	17.001(11)	16.955(11)	16.8665(2)
P_γ (u Å^2)	2.743(9)	2.780(10)	2.759(1)	2.713(11)	3.4919(2)
Δ_0 [b]	1.498(18)	1.424(20)	1.465(22)	1.558(22)	–

[a] For the complexes $C_2H_4\cdots HBr$, the identification $\alpha = a$, $\beta = b$ and $\gamma = c$ should be made but for free C_2H_4 the appropriate identification is $\alpha = c$, $\beta = a$ and $\gamma = b$.
[b] Δ_0 is the pseudo-inertia defect of $C_2H_4\cdots HBr$ defined in Eq. (7).

$$P_b^E = (1/2)(I_a + I_c - I_b) = 4m_H b_H^2 \quad (5)$$

where b_H is the distance of the H atoms in ethene from the *ac* plane (see Fig. 1 for a diagram of the principal inertia axes of ethene). Correspondingly, it is possible to express P_c of the complex as

$$P_c = (1/2)(I_a^0 + I_b^0 - I_c^0) = -(1/2)\Delta_0 + 4m_H c_H^2 \quad (6)$$

where Δ_0 is the pseudo-inertia defect of the complex in the ground-state, i.e. the inertia defect remaining after the out-of-plane contribution of the four H atoms is subtracted from P_c. But the *b* axis of ethene is parallel to the *c* axis of the complex (see Fig. 1) and therefore we can replace $4m_H c_H^2$ in Eq. (6) by P_b^E to give

$$P_b^E - P_c = (1/2)\Delta_0 \quad (7)$$

Values of Δ_0 calculated from Eq. (7) are given in Table 5. The relatively large variation among the isotopomers reflects the poor determination of the rotational constant A_0. We note that the mean value $\Delta_0 = 1.49(6)$ u Å^2 should be compared with the inertia defect 1.2(3) u Å^2 of the planar T-shaped complex $C_2H_2\cdots HCl$ [14].

Having established that the $C_2H_4\cdots HBr$ has C_{2v} symmetry and the equilibrium angular geometry shown in Fig. 1, it remains to determine the distance $r(*\cdots Br)$ from the centre (*) of the C=C bond to Br. The changes in the rotational constants B_0 and C_0 of $C_2H_4\cdots H^{79}Br$ on isotopic substitution at H and Br in HBr (see Table 2) show that H lies closer to the complex centre of mass than does Br. Hence, the system defined by the three points $*\cdots H-Br$ lies in the indicated order and the interaction is a hydrogen bond. It will be shown in Section 5 that the intermolecular stretching force constant k_σ, determined from the centrifugal distortion constant Δ_J, indicates weak binding. This suggests that it is a reasonable approximation to assume the geometries and principal moments of inertia of the free molecules C_2H_4 and HBr (see Table 4) are unchanged in the complex.

It is readily shown that, for the geometry given in Fig. 1, the equilibrium principal moments of inertia of the complex I_α are related to those of free ethene, I_α^E, and free HBr, I_b^{HBr}, through Eqs. (8)–(10):

$$I_a = I_c^E \tag{8}$$

$$I_b = \mu r_{cm}^2 + I_a^E + I_b^{HBr} \tag{9}$$

$$I_c = \mu r_{cm}^2 + I_b^E + I_b^{Hbr} \tag{10}$$

where r_{cm} is the distance between the centres of mass of the ethene and HBr subunits and $\mu = m^E m^{HBr}/(m^E + m^{HBr})$. Only zero-point moments of inertia are available from this work and, to utilise these, Eqs. (8)–(10) need to be modified to allow for zero-point effects. Some progress is possible in this respect for the HBr subunit via the Br nuclear quadrupole coupling constants.

We describe, as is customary, the contribution of the HBr subunit to the zero-point motion in terms of the HBr angular oscillation pivoted at its mass centre, as illustrated in Fig. 2. The small difference $\chi_{bb} - \chi_{cc}$ in the Br nuclear quadrupole coupling constants associated with the *b* and *c* directions (see Table 2) provides evidence that to a good approximation the motion is two-dimensionally isotropic in the *bc* plane. Hence, the motion in the angle ψ describes a circle. If the additional electric field gradient at Br that arises from the presence of the ethene electric charge distribution is negligible, a measure of the average value $\langle \cos^2 \theta \rangle$,

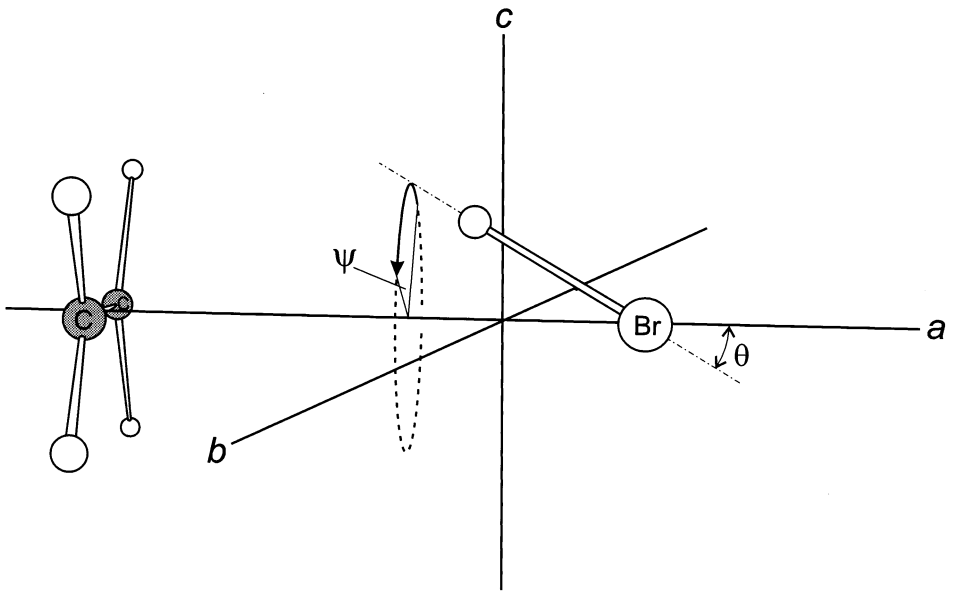

Fig. 2. The model of $C_2H_4 \cdots HBr$ used to determine the geometry of the complex from its zero-point moments of inertia. The angular oscillation of the HBr subunit illustrated is two-dimensionally isotropic in the *bc* plane and is defined in terms of the angles ψ and θ. This diagram is drawn to scale, except for the angle θ, which is exaggerated with respect to $\theta_{av} = \cos^{-1}\langle \cos^2 \theta \rangle^{1/2}$, determined from χ_{aa}, for clarity.

Table 6
Some properties of the isotopomers $C_2H_4\cdots H^{79}Br$, $C_2H_4\cdots H^{81}Br$, $C_2H_4\cdots D^{79}Br$, $C_2H_4\cdots D^{81}Br$ of the ethene–hydrogen bromide complex

Property		$C_2H_4\cdots H^{79}Br$	$C_2H_4\cdots H^{81}Br$	$C_2H_4\cdots D^{79}Br$	$C_2H_4\cdots D^{81}Br$
θ_{av} (deg) [a]		21.015(1)	21.011(1)	19.032(1)	19.030(1)
r_{cm} (Å) [b]	I_b	3.8970	3.8974	3.8761	3.8760
	I_c	3.9026	3.9029	3.8815	3.8813
r(*···Br) (Å) [b]	I_b	3.9150	3.9146	3.9115	3.9105
	I_c	3.9205	3.9201	3.9169	3.9159
k_σ (N m^{-1}) [c]		5.19 (1)	5.24 (1)	5.45 (1)	5.42 (1)

[a] Determined from the Br nuclear quadrupole coupling constant χ_{aa} by using Eq. (11).
[b] Distances in the row labelled I_b were determined from Eq. (12), while Eq. (13) was used for the values in the row labelled I_c.
[c] Determined from Δ_J by using Eq. (15).

where θ is the other oscillation angle (see Fig. 2), is available from the coupling constant χ_{aa} according to the familiar expression

$$\chi_{aa} = (1/2)\chi_0\langle 3\cos^2\theta - 1\rangle \tag{11}$$

where χ_0 is the Br nuclear quadrupole coupling constant of free HBr or DBr [15,16] and its values are given in Table 4. Values of $\theta_{av} = \cos^{-1}\langle\cos^2\theta\rangle^{1/2}$ calculated using Eq. (11) with the χ_{aa} from Table 2 are given in Table 6. Note that θ_{av} is smaller for the DBr complexes, as required by the greater reduced mass for the angular motion of the DBr subunit.

It is readily shown that, if the motion of the HBr subunit depicted in Fig. 2 is taken into account, Eqs. (9) and (10) become

$$I_b = \mu r_{cm}^2 + I_a^E + (1/2)I_b^{HBr}\langle 1 + \cos^2\theta\rangle \tag{12}$$

and

$$I_c = \mu r_{cm}^2 + I_b^E + (1/2)I_b^{HBr}\langle 1 + \cos^2\theta\rangle \tag{13}$$

Since we have no information about the angular oscillation of the ethene subunit in the zero-point state of the complex from a similar source, it is not possible to make the corresponding modification of the terms I_a^E and I_b^E in these equations. Instead, they remain as equilibrium values. It should be noted that, in deriving Eqs. (12) and (13), the intermolecular stretching motion has been ignored, so that r_{cm} is taken as fixed.

Values of r_{cm} obtained by using the moments of inertia of ethene, HBr and the complex in each of Eqs. (12) and (13) are recorded in Table 6. Zero point values of I_a^E, I_b^E and I_b^{HBr}, which are available from the rotational constants [13,17] given in Table 4, were used in place of equilibrium quantities. Also included in Table 6 are the distances r(*···Br) from the centre of the C=C bond to Br, which can be obtained from r_{cm} with the aid of the expression

$$r(*\cdots Br) = r_{cm} + r \tag{14}$$

where r is the distance of the HBr mass centre from the Br atom. Some measure of the contribution of zero-point effects to the distance $r(*\cdots Br)$ is available from the difference in this quantity when determined from I_b and I_c (i.e. from Eqs. (12) and (13), respectively). For a given isotopomer, this difference is ca. 0.005 Å. On the other hand, the isotopic dependence of $r(*\cdots Br)$ can be gauged by examining the values determined via I_b, for example. It is clear from Table 6 that although $r(*\cdots Br)$ is effectively unchanged by ^{81}Br substitution, the effect of substituting D in $H^{79}Br$ is to shorten the distance by ca. 0.004 Å. Such shortenings of hydrogen bonds on D/H substitution in gas-phase complexes are not uncommon [18].

5. Strength of intermolecular binding

One property of the weakly bound complex that provides a measure of the strength of the intermolecular binding is the quadratic force constant k_σ, i.e. the restoring force per unit infinitesimal displacement along the hydrogen bond direction. Under the assumption of rigid unperturbed subunits B and HX involved in a complex in which the axis of the diatomic molecule HX is perpendicular to the plane of the nuclei in a planar base B, Millen has shown that k_σ is related to the centrifugal distortion constant Δ_J by the expression [19]:

$$k_\sigma = (8\pi^2\mu/\Delta_J)\{B^3(1-b) + C^3(1-c)\} \tag{15}$$

In Eq. (15), B and C are rotational constants of the complex, μ is the quantity introduced in Eqs. (9) and (10), while $b = (B/B_B + B/B_{HX})$ and c has the corresponding definition in terms of the rotational constants C, C_B and C_{HX}. Strictly, the rotational constants in Eq. (15) should be equilibrium values but these are unavailable and zero-point values, from Table 2 for ethene···HBr and Table 4 for ethene [13] and HBr [17], have been used instead. The resulting k_σ values of the four isotopomers of ethene···HBr investigated are included in Table 6. We note that, while there is agreement between k_σ of the two isotopomers involving HBr and between the two isotopomers based on DBr, the deuterium-bonded complexes are significantly more strongly bound, according to the k_σ criterion, than the hydrogen-bonded complexes. This effect is consistent with the shorter distances $r(*\cdots Br)$ for DBr species, as discussed in Section 4, and has been noted [18] for several types of complex B···HX.

6. Discussion

A complex formed between ethene and hydrogen bromide has been observed in the gas phase by using a fast-mixing nozzle to avoid any reaction between the components that might be initiated through production of Br atoms on the surface of a vessel when they are mixed conventionally. The ground-state rotational spectra

of four isotopomers of $C_2H_4\cdots HBr$ were observed in supersonic expansions by the Fourier-transform microwave technique conducted in a Fabry-Pérot cavity. Analyses of rotational constants, centrifugal distortion constants and Br nuclear quadrupole coupling constants led to the conclusion that the HBr interacts with ethene through a weak hydrogen bond. The observed complex has an equilibrium geometry in which the HBr subunit lies along the C_2 axis that is perpendicular to the plane of the nuclei in ethene. The observed geometry is that expected if $^{\delta+}$H of HBr seeks out the most nucleophilic region of ethene, with the internuclear axis of HBr lying along the symmetry axis of the π orbital. Thus, $C_2H_4\cdots HBr$ is isostructural with all other complexes of the general type $C_2H_4\cdots HX$ and $C_2H_4\cdots XY$, where X and Y are halogen atoms, so far investigated in the gas phase [20–24].

In addition to the chemical challenge of isolating and characterising a complex $C_2H_4\cdots HBr$, there was another reason for this investigation. This reason concerns the distance $r(*\cdots Br)$ between the centre (*) of the C=C bond and the Br atom and its relationship to the corresponding distance in $C_2H_4\cdots BrCl$. In particular, we seek to answer the question: Does the difference Δr in this distance fit the pattern established earlier [25] for four other pairs of complexes B···HBr/B···BrCl?

Table 7 compares the distances $r(Z\cdots Br)$ and, their differences Δr, in B···HBr and B···BrCl for B = CO [26,27], C_2H_4 [23], H_2S [28,29], HCN [30,31] and NH_3 [32,33]. Included are the intermolecular stretching force constants k_σ to provide a measure of binding strength. We note from Table 7 that Δr is substantial for each B and that it decreases as the binding strength increases. The behaviour of the corresponding series $B\cdots HCl/B\cdots Cl_2$, the values of $r(Z\cdots Cl)$, Δr and k_σ for which [2] are also given in Table 7, is remarkably similar, except that the contraction Δr between B···HCl and $B\cdots Cl_2$ is somewhat smaller than between B···HBr and B···BrCl. For example, the expression $\Delta r(B\cdots HBr/\ B\cdots BrCl) = 1.58(3)\ \Delta r(B\cdots HCl/B\cdots Cl_2)$ holds for each B. Evidently, the conclusions about the 'snub-nosed' nature of the Cl_2 molecule, identified experimentally [2,3] and by ab initio calculations [5], and discussed in the Introduction, also apply to BrCl. The fact that the contraction Δr from B···HX to B···XY is larger by 0.31(5) Å for the series X = Br than the series X = Cl (see Table 7) presumably reflects in part the excess of the Van der Waals radius of the Br atom, $\sigma(Br) = 1.95$ Å, over that of the Cl atom, $\sigma(Cl) = 1.80$ Å. Ab initio calculations in which the He atom is used to probe the repulsive potential lead to values of $\Delta r = 0.60$ Å [5] and 0.71 Å [34] for $B\cdots HCl/B\cdots Cl_2$ and B···HBr/B···BrCl, respectively.

Finally, we note from Table 7 that systematic relationships exist among the k_σ values. For example, the ratio $k_\sigma(B\cdots BrCl)/k_\sigma(B\cdots Cl_2) = 1.84(16)$ holds for all B while $k_\sigma(B\cdots HCl)/k_\sigma(B\cdots HBr) = 1.24(10)$. By examining complexes B···HX for a wide range of Lewis bases B and acids HX = HF, HCl, HBr, HCN, HCCH, an empirical expression [35,36]

$$k_\sigma = cN_B E_{HX} \tag{16}$$

was established in which N_B is the gas-phase nucleophilicity of B, E_{HX} is the gas-phase electrophilicity of HX, and c is a constant. Since $C_2H_4\cdots HBr$ was not used to generate the scale of nucleophilicities and electrophilicities, we can use the

Table 7
Comparison of distances $r(Z\cdots X)$ [a] and intermolecular stretching force constants k_σ in the series B···HX and B···XY, where X = Br or Cl and Y = Cl

B	B···HBr		B···BrCl			B···HCl [b]		B···Cl_2 [b]		
	$r(Z\cdots Br)$ (Å)	k_σ (Nm^{-1})	$r(Z\cdots Br)$ (Å)	k_σ (Nm^{-1})	Δr (Å)	$r(Z\cdots Cl)$ (Å)	k_σ (Nm^{-1})	$r(Z\cdots Cl)$ (Å)	k_σ (Nm^{-1})	Δr (Å)
OC	3.917 [c]	3.0 [d]	3.004 [e]	6.3 [e]	0.91	3.710	3.9	3.134	3.7	0.58
C_2H_4	3.916 [f]	5.2 [f]	2.979 [g]	10.5 [g]	0.94	3.724	5.9	3.128	5.8	0.60
H_2S	3.991 [h]	5.9 [h]	3.096 [i]	12.1 [i]	0.90	3.809	6.8	3.249	6.3	0.56
HCN	3.610 [j]	7.3 [k]	2.834 [l]	11.2 [l]	0.78	3.405	9.1	2.915	6.6	0.49
NH_3	3.255 [m]	13.1 [m]	2.628 [n]	26.7 [n]	0.63	3.136	18.2	2.724	12.7	0.41

[a] Z is the electron donor centre in B (i.e. either the atom carrying the appropriate nonbonding electron pair or the centre of the π bond).
[b] For a convenient summary of $r(Z\cdots Cl)$ and k_σ values in the series B···HCl and B···Cl_2, see Ref. [2].
[c] Recalculated from data in Ref. [26] by method described in Ref. [18].
[d] Recalculated from D_J given in Ref. [26] by method described in Ref. [19].
[e] Ref. [27].
[f] This work.
[g] Ref. [24].
[h] Ref. [28].
[i] Ref. [29]
[j] Recalculated from data in Ref. [30] by method described in Ref. [18].
[k] Recalculated from D_J given in Ref. [30] by method described in Ref. [19].
[l] Ref. [31].
[m] Ref. [32].
[n] Ref. [33].

values $N_{C_2H_4} = 4.7$ [36] and $E_{HBr} = 4.2$ [35] thereby established when $c = 0.25$ Nm^{-1} to test further Eq. (16). The result k_σ (C_2H_4···HBr) = 5.0 Nm^{-1} so calculated is in satisfactory agreement with that observed [5.19(1) Nm^{-1}, see Table 6]. A scale of electrophilicities E_{XY} for dihalogen molecules has also been established [37] on the basis of k_σ values for a wide range of B···XY complexes.

Acknowledgements

The authors would like to thank the Leverhulme Trust and the Exeter University Research Committee for financial support of this work. ACL thanks to EPSRC for a Senior Fellowship. We are grateful to James Davey for help with some computing.

References

[1] A.C. Legon, C.A. Rego, J. Chem. Soc. Faraday Trans. 86 (1990) 1915.
[2] A.C. Legon, Chem. Phys. Lett. 237 (1995) 291.
[3] H.I. Bloemink, K. Hinds, A.C. Legon, J.C. Thorn, Chem. Phys. Lett. 223 (1994) 162.
[4] A.C. Legon, Chem. Phys. Lett. 279 (1997) 55.
[5] S.A. Peebles, P.W. Fowler, A.C. Legon, Chem. Phys. Lett. 240 (1995) 130.
[6] T.J. Balle, W.H. Flygare, Rev. Sci. Instrum. 52 (1981) 33.
[7] A.C. Legon, in: G. Scoles (Ed.), Atomic and Molecular Beam Methods, vol. 2, Oxford University Press, New York, 1992, p. 289.
[8] H.M. Pickett, J. Mol. Spectrosc. 148 (1991) 371.
[9] M.R. Keenan, E.J. Campbell, T.J. Balle, L.W. Buxton, T.K. Minton, P.D. Soper, W.H. Flygare, J. Chem. Phys. 72 (1980) 3070.
[10] L.C. Willoughby, A.C. Legon, J. Phys. Chem. 87 (1983) 2085.
[11] J. Hougen, J. Chem. Phys. 57 (1972) 4207.
[12] A.C. Legon, J.C. Thorn, Chem. Phys. Lett. 215 (1993) 554.
[13] F. Herlemont, M. Lyszyk, J. Lemaire, Ch. Lambeau, M. de Vleeschouwer, A. Fayt, J. Mol. Spectrosc. 94 (1982) 309.
[14] A.C. Legon, P.D. Aldrich, W.H. Flygare, J. Chem. Phys. 75 (1981) 625.
[15] O.B. Dabbousi, W.L. Meerts, F.H. Deleeuw, A. Dymanus, Chem. Phys. 2 (1973) 473.
[16] F.A. Van Dijk, A. Dymanus, Chem. Phys. 6 (1974) 474.
[17] F.C. DeLucia, P. Helminger, W. Gordy, Phys. Rev. 3 (1971) 1849.
[18] A.C. Legon, D.J. Millen, Chem. Phys. Lett. 147 (1988) 484.
[19] D.J. Millen, Can. J. Chem. 63 (1985) 1477.
[20] J.A. Shea, W.H. Flygare, J. Chem. Phys. 76 (1982) 4857.
[21] P.D. Aldrich, A.C. Legon, W.H. Flygare, J. Chem. Phys. 75 (1981) 2126.
[22] H.I. Bloemink, J.H. Holloway, A.C. Legon, Chem. Phys. Lett. 250 (1996) 257.
[23] H.I. Bloemink, K. Hinds, A.C. Legon, J.C. Thorn, Chem. Eur. J. 1 (1995) 17.
[24] H.I. Bloemink, K. Hinds, A.C. Legon, J.C. Thorn, Angew. Chem. Intl. Ed. Engl. 33 (1994) 1512.
[25] A.C. Legon, J. Chem. Soc. Faraday Trans. 91 (1995) 1881.
[26] M.R. Keenan, T.K. Minton, A.C. Legon, T.J. Balle, W.H. Flygare, Proc. Natl. Acad. Sci. USA 77 (1980) 5583.
[27] S. Blanco, A.C. Legon, J.C. Thorn, J. Chem. Soc. Faraday Trans. 90 (1994) 1365.
[28] A.I. Jaman, A.C. Legon, J. Mol. Struct. 145 (1986) 261.
[29] H.I. Bloemink, A.C. Legon, Chem. Eur. J. 2 (1996) 265.

[30] E.J. Campbell, A.C. Legon, W.H. Flygare, J. Chem. Phys. 78 (1983) 3494.
[31] K. Hinds, A.C. Legon, Chem. Phys. Lett. 240 (1995) 467.
[32] N.W. Howard, A.C. Legon, J. Chem. Phys. 86 (1987) 6722.
[33] H.I. Bloemink, A.C. Legon, J.C. Thorn, J. Chem. Soc. Faraday Trans. 91 (1975) 781.
[34] S.A. Peebles, P.W. Fowler, A.C. Legon, unpublished calculations.
[35] A.C. Legon, D.J. Millen, J. Am. Chem. Soc. 109 (1987) 356.
[36] A.C. Legon, D.J. Millen, J. Chem. Soc. Chem. Commun. (1987) 986.
[37] A.C. Legon, J. Chem. Soc. Chem. Commun. (1998) 2585.